Nuclear Engineering and Technology 48 (2016) 831–839

Available online at ScienceDirect

Nuclear Engineering and Technology

journal homepage: www.elsevier.com/locate/net

Original Article

A Time-Domain Method to Generate Artificial Time History from a Given Reference Response Spectrum

Gangsig Shin [a,b] and Ohseop Song [b,*]

[a] Korea Institute of Nuclear Safety, 62 Gwahak-ro, Yuseong-gu, Daejeon 34142, South Korea
[b] Department of Mechanical Engineering, Chungnam National University, 99 Daehak-ro, Yuseong-gu, Daejeon 34134, South Korea

ARTICLE INFO

Article history:
Received 14 October 2015
Received in revised form
22 January 2016
Accepted 25 January 2016
Available online 24 March 2016

Keywords:
Artificial Time History
Response Spectrum
Seismic Qualification
Time-Domain Peak Reduction

ABSTRACT

Seismic qualification by test is widely used as a way to show the integrity and functionality of equipment that is related to the overall safety of nuclear power plants. Another means of seismic qualification is by direct integration analysis. Both approaches require a series of time histories as an input. However, in most cases, the possibility of using real earthquake data is limited. Thus, artificial time histories are widely used instead. In many cases, however, response spectra are given. Thus, most of the artificial time histories are generated from the given response spectra. Obtaining the response spectrum from a given time history is straightforward. However, the procedure for generating artificial time histories from a given response spectrum is difficult and complex to understand. Thus, this paper presents a simple time-domain method for generating a time history from a given response spectrum; the method was shown to satisfy conditions derived from nuclear regulatory guidance.

1. Introduction

Since the great earthquake in east Japan, the safety of nuclear power plants against earthquakes has been a critical concern. To guarantee the safety of nuclear power plants against earthquakes, each system, structure, and component that is important to safety must maintain its structural integrity and perform its designated safety function. For any of these components or equipment, the integrity and/or functionality can be evaluated using seismic qualification by test or analysis. To use the qualification by test method, the time history for the seismic input to the shake table is needed. Likewise, time history is required when using the qualification by direct integration analysis method, as an input to the analysis.

However, in most cases, using time histories from actual earthquake data has many limitations for many reasons. Hence, artificial time history sets, generated from response spectra, are widely used instead. The methods used to generate time histories have been studied by many researchers. Kost et al. [1] defined an initial seismic time history using the concept of Fourier series coefficients, and used the ratio between a given design response spectrum and the

* *Corresponding author.*
E-mail address: songos@cnu.ac.kr (O. Song).
http://dx.doi.org/10.1016/j.net.2016.01.023

computed response spectrum to get the time history. They generated artificial time histories that follow the target response spectrum up to 20 Hz. Levy and Wilkinson [2] used time histories with phase angles of 0° and 180° only, and studied the effect of the frequency step (number of data points in the same frequency range) on the accuracy of the computed resultant response spectrum. Jun et al. [3] proposed a method that can make use of information on general buildings to generate artificial time histories. Tsai [4] and Rizzo et al. [5] researched a method to obtain smoother computed response spectra using local suppressing and raising techniques. Deviating from the above methods, which are deterministic, Vanmarcke [6] developed a random vibration method using a spectral density function, and this method had been updated to develop a computer program [7] to generate artificial time histories. Aziz and Biswas [8] reviewed time history-generating methods and applied them to the seismic analysis of a typical CANadia Deuterium Urinium (CANDU) nuclear power plant reactor building. However, some of those methods are applicable only to general buildings so that they cannot meet the regulatory requirements for nuclear application, and some of them are difficult to apply in field applications. Therefore, in this study, a new method to modify the artificial time history in the time domain is used to generate a response spectrum that matches a given reference response spectrum and meets conditions derived from the regulatory requirements at the same time.

2. Response spectra

In many cases, an artificial seismic time history is generated from a response spectrum that is defined in a design specification or regulatory guidance. A response spectrum is a conceptual spectrum that is different from the Fourier spectrum of time history. It is a series of maximum time history responses of one-degree-of-freedom (dof) systems having different natural frequencies. The basic concept of the response spectrum is shown in Fig. 1.

The first graph in Fig. 1 is an example of a portion of base excitation data. The second picture of Fig. 1 represents a set of one-dof systems with different natural frequencies. Once the ground acceleration of (A) is applied to the array of systems of (B), then each time history response at each one-dof system can be acquired as shown in (C). Here, the response spectrum can be acquired by plotting the maximum absolute value from each time history response of (C). at a corresponding frequency, as shown in (D). Therefore, the resultant response spectrum is completely different from a simple Fourier spectrum.

If the ground acceleration is $\ddot{x}(t)$, then the maximum pseudoacceleration of the response time history at ω_n can be written as follows [9]:

$$S_{pa}(\omega_n) = |\ddot{x}(t)*h(\omega_n,t)|_{\max} = \left|\int \ddot{x}(t)h(4\omega_n, t-\tau)d\tau\right|_{\max} \quad (1)$$

Here, the operator * denotes the convolution integral, and $h(\omega_n,t)$ is the one-dof system impulse response at the natural frequency ω_n, with fraction of critical damping ξ.

From Eq. (1), one can get the response spectrum simply by plotting the maximum response value, S_{pa}, as a function of ω_n on the $\omega \times S_{pa}$ plane, as shown in (D) of Fig. 1. Hence, the response spectrum can be generated using both information about input, $\ddot{x}(t)$, and the one-dof system, $h(\omega_n,t)$, simultaneously, while the simple Fourier spectrum reflects only the frequency characteristic of $\ddot{x}(t)$ or $h(\omega_n,t)$. Therefore, the response spectrum is a readily calculated array of maximum responses of a one-dof system to a certain seismic input, while the Fourier spectrum of input $\ddot{x}(t)$ shows the frequency contents of the input itself.

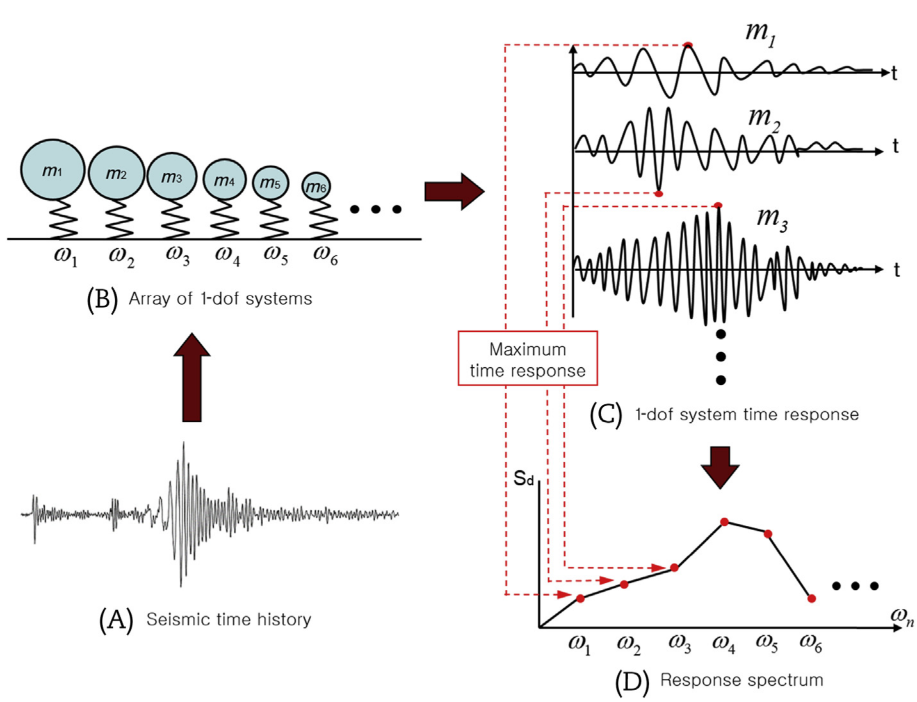

Fig. 1 – Basic concept of response spectrum. dof, degree of freedom.

As one can see from Eq. (1), calculating the response spectrum from a given time history is straightforward. However, deriving artificial time histories from a given response spectrum can be far more difficult. In many cases, they provide designers only with response spectra for component design. However, the given response spectrum is nothing but a series of maximum acceleration values as a function of natural frequency, as described in Fig. 1. Therefore, the given response spectrum does not contain important information such as phase angle. Moreover, thousands of artificial time histories can be derived from the given response spectrum. Hence, in practice, ready-made computer programs such as SIMQKE are used [7] to generate artificial time histories.

3. Time history generation from a given response spectrum

3.1. *Regulatory guidance*

Many response spectra can be used as reference response spectra. In many cases, reference response spectra are provided in the design specifications. For nuclear power plants, in particular, ground response spectra recommended by the United States Nuclear Regulatory Commission are used in most cases.

These ground response spectra are mentioned in Regulatory Guide 1.60 revision 1 [10], which provides two sets of response spectra scaled to 1*g* peak ground acceleration. One is for horizontal design response spectra and the other for vertical design response spectra. Each set contains five response spectra with different damping factors. As an example, the horizontal design response spectra presented in Regulatory Guide 1.60 is shown in Fig. 2.

While Regulatory Guide 1.60 gives reference response spectra, Section 3.7.1 of NUREG-0800 (NUREG series are reports on regulatory decisions by US Nuclear Regulatory Commission) gives technical guidance on artificial time history generation. In Revision 3 of NUREG-0800 Section 3.7.1 [11], a second approach to generate the artificial time history was added, which does not require power spectrum density calculation. Thus, in this study, to avoid power spectrum density calculation, the new guidance from Revision 3 of NUREG-0800 Section 3.7.1, "SRP Acceptance criteria 1.B∖Option 1∖Approach 2," which is effective in Korea, is used. From the regulatory guidance in Section 3.7.1 of NUREG-0800 Revision 3, the following items can be applied to this case. These items are chosen and modified to meet the purpose of this study. (1) The artificial time history should have a peak acceleration identical to the peak ground acceleration of the site. (2) The strong motion duration is defined as the time required for the Arias intensity to rise from 5% to 75%, and should be longer than 6 seconds. (3) Spectral acceleration at

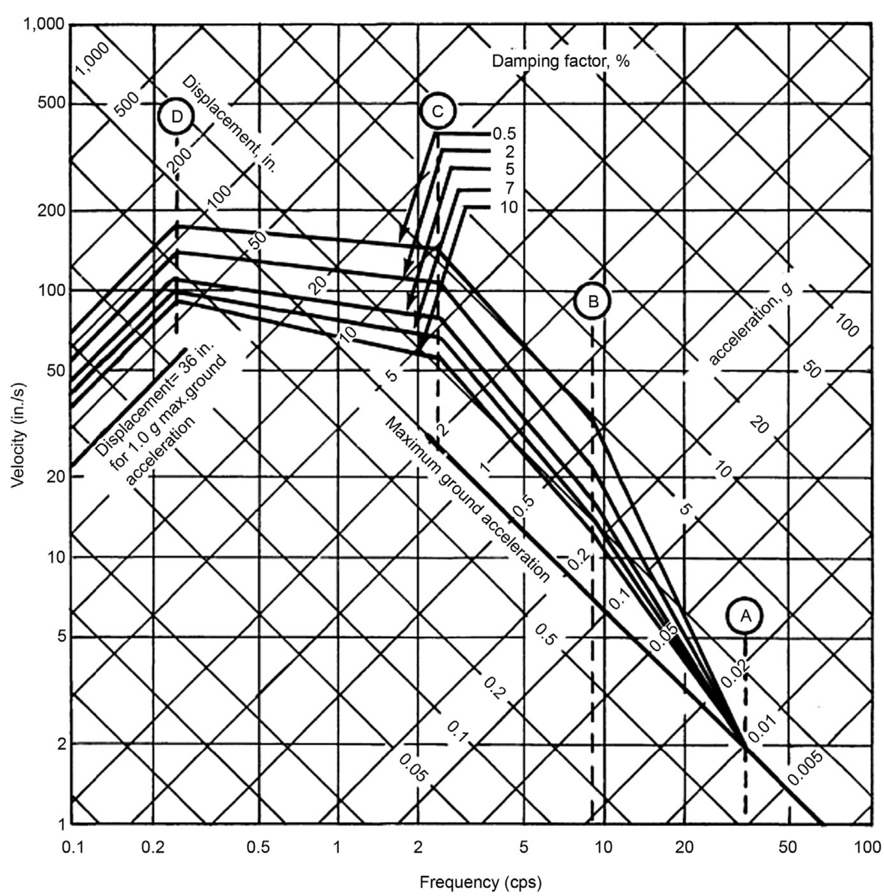

Fig. 2 – Ground response spectrum given by Regulatory Guide 1.60.

5% damping shall be computed from 0.1 Hz to 50 Hz or the Nyquist frequency. The comparison of the response spectrum obtained from the artificial ground motion time history with the target response spectrum shall be made at each frequency computed in the frequency range of interest. (4) Records shall have a Nyquist frequency of at least 50 Hz (e.g., a time increment of a maximum of 0.010 seconds) and a total duration of at least 20 seconds. (5) The computed 5%-damped response spectrum of the accelerogram shall not fall more than 10% below the target response spectrum at any one frequency. To prevent response spectra in large-frequency windows from falling below the target response spectrum, the response spectra within a frequency window of no larger than ±10% centered on the frequency shall be allowed to fall below the target response spectrum. This corresponds to response spectra at no more than nine adjacent frequency points, defined in (3) above, falling below the target response spectrum. (6) In lieu of the power spectrum density requirement of Approach 1, the computed 5%-damped response spectrum of the artificial ground motion time history shall not exceed the target response spectrum at any frequency by > 30% (a factor of 1.3) in the frequency range of interest.

As defined in Regulatory Guide 1.60, there is more than one response spectrum curve. In practice, two horizontal curves (normally in N–S and E–W directions) and one vertical curve are used. Hence, there is an additional regulatory guidance in Section 3.7.1 of NUREG-0800, such as a correlation check between the three directional results. However, because the topic of this paper is restricted to the generation of an artificial time history from a given response spectrum, only one response spectrum and the corresponding time history will be covered here. Therefore, in this study, the horizontal ground response spectrum with $\zeta = 5\%$ is used as the reference response spectrum.

3.2. *Initial time history*

An acceleration time history $\ddot{x}(t)$ can be represented as a sum of N sinusoids of magnitude A_n at an angular frequency ω_n having a phase angle φ_n:

$$\ddot{x}(t) = \sum_{n=1}^{N} A_n \sin(\omega_n t + \varphi_n) \tag{2}$$

To form an initial time history, the response spectrum acceleration at ω_n of the reference response spectrum is used as the magnitude A_n of $\ddot{x}(t)$. The phase angle φ_n can be chosen randomly between 0 and 2π. A sample initial time history prepared by Eq. (2) is shown in Fig. 3.

In reality, the earthquake gradually increases its magnitude, holds its maximum magnitude for some time, and then fades out. Therefore, to generate more realistic characteristics of earthquake acceleration, an envelope function containing build-up, intense motion (or strong motion), and decay is adopted as a reference [7]. Some types of envelope functions are shown in reference [7]. If the envelope function is defined as $I(t)$, then Eq. (2) can be redefined as follows:

$$\ddot{x}(t) = I(t) \sum_{n=1}^{N} A_n \sin(\omega_n t + \varphi_n) \tag{3}$$

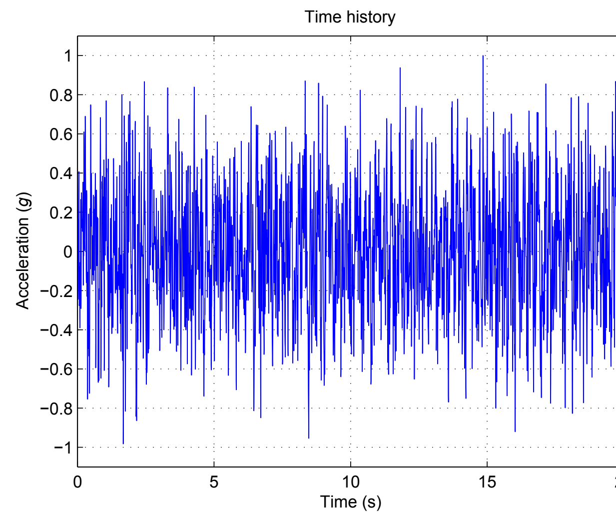

Fig. 3 – Time history plot by Eq. (2).

A sample initial time history with an envelope function applied to the time history in Fig. 3 is shown in Fig. 4. Here, to satisfy the first of the six conditions in Section 3.1, the maximum value of the artificial time history is scaled to unity because the peak ground acceleration (acceleration response above the cut-off frequency, 33 Hz) in Fig. 2 is 1*g*. During the iteration, before calculating each response spectrum, the time history is scaled again to meet this condition. The envelope function can be chosen from [7]. Here, to meet the second condition for obtaining the artificial time history stated in Section 3.1, a strong motion is chosen to start at 1 second and to last until 15 seconds, which is longer than 6 seconds. Like the scaling above, enveloping is conducted at each iteration before calculating each response spectrum.

In this study, the sampling rate is 200 times/s and the total number of samples is 4,000, which means that the time-domain sampling interval in the artificial time history is equal to 0.005 seconds and the total duration of the time history is 20 seconds. This corresponds to a Nyquist frequency of 100 Hz with a duration of 20 seconds, satisfying the fourth

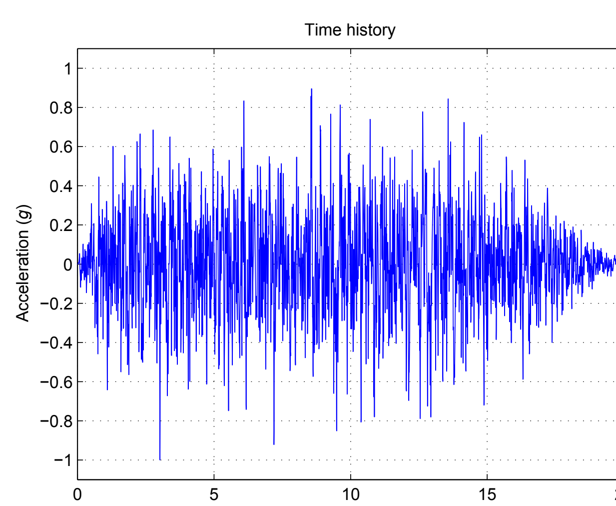

Fig. 4 – Time history plot by Eq. (3).

condition in Section 3.1. Additionally, this study uses a series of one-dof systems with 5% damping and aims to meet the 5% damping reference response spectrum. The frequency range for the calculation is from 0.05 Hz to 50 Hz, which meets the third condition for the artificial time history.

Among the six conditions for the artificial time history to satisfy the guidance in reference [11], Conditions 1, 2, 3, and 4 deal with the time domain, while the others are related to the frequency domain. At this point in the paper, the four conditions dealing with the time domain are met. The remaining two conditions will be covered in the next section.

3.3. *Response spectrum matching*

Once the initial input time history $\ddot{x}(t)$ has been defined, it is applied to the series of one-dof systems. We can then obtain the initial calculated response spectrum (CRS) corresponding to the initial time history using Eq. (1). However, direct calculation of convolution requires substantial computational resources and time. Moreover, to match the target reference response spectrum, an iterative process is essential. Therefore, calculating the convolution integral throughout the iteration is not an effective approach. However, the convolution integral can be calculated easily in the frequency domain. Thus, in this study, calculations are conducted in the frequency domain.

The Fourier transform of $\ddot{x}(t)$ and that of one-dof system $h(\omega_n,t)$ are, respectively, as follows:

$$\ddot{X}(\omega) = \int \ddot{x}(t)e^{-j\omega t}dt \tag{4}$$

$$H(\omega_n, \omega) = \int h(\omega_n, t)e^{-j\omega t}dt \tag{5}$$

The convolution integral, Eq. (1), can be calculated by simple multiplication of $\ddot{X}(\omega)$ and $H(\omega_n,\omega)$, followed by inverse Fourier transform. This can be expressed as follows:

$$S_{pa}(\omega_n) = |\ddot{x}(t)*h(\omega_n,t)|_{max} = \left|F^{-1}\{\ddot{X}(\omega)H(\omega_n,\omega)\}\right|_{max} \tag{6}$$

where $F^{-1}\{A(\omega)\}$ denotes inverse Fourier transform of $A(\omega)$.

The pseudoacceleration S_{pa} at ω_n must be calculated throughout the frequency range of interest. This provides the initial CRS. However, at this stage, the initial CRS does not match the reference response spectrum. An iterative process that can closely match the CRS to the required response spectrum (RRS) is therefore required. In this study, the RRS is the 5% damping ground response spectrum given in Fig. 2. During iteration, the magnitudes of the sinusoids in Eq. (3) are modified to obtain an optimized set of A_n. The ratio between the RRS and the CRS can be denoted as follows:

$$R(\omega_n, \xi) = \frac{CRS(\omega_n, \xi)}{RRS(\omega_n, \xi)} \tag{7}$$

The magnitude of the new time history at step $(k+1)$ can now be calculated by the following equation:

$$A_{n,k+1} = \frac{A_{n,k}}{R(\omega_n, \xi)} \tag{8}$$

Now, with the new magnitude for step $(k+1)$ set to $A_{n,k+1}$, the time history for step $(k+1)$, $\ddot{x}(t)_{k+1}$, can once again be obtained by Eq. (3). After that, the new CRS at step $(k+1)$ can be acquired, which leads to a new response spectrum ratio at step $(k+1)$. Through this iterative process, a time history that can obtain a response spectrum that approaches the reference response spectrum can be generated. Results calculated from the initial time history in Fig. 4 are shown in Figs. 5–7. Fig. 5 shows the CRS and its target (RRS), while Fig. 6 shows the time history for getting the CRS in Fig. 5. Fig. 7 shows the ratio between the CRS and the RRS to check if it meets the conditions in the frequency domain (Conditions 5 and 6 in Section 3.1). As can be seen from Fig. 7 and the work of Levy and Wilkinson [2], the ratio between the CRS and the RRS in the high-frequency region is much higher than that in the low-frequency region. This is because, as Levy and Wilkinson [2] mentioned in their work, the high-frequency region (beyond resonance) response spectrum value of a single sinusoidal input with unit peak amplitude approaches unity, as depicted in Fig. 8. Moreover, if we combine Eqs. (3) and (1), then the pseudoacceleration response spectrum can be written as follows:

$$\begin{aligned} S_{pa}(\omega_n) &= \left|\int \ddot{x}(t)h(t-\tau)d\tau\right|_{max} \\ &= \left|\int \left(I(t)\sum_{m=1}^{N} A_m \sin(\omega_m t + \varphi_m)\right)h(t-\tau)d\tau\right|_{max} \\ &= \left|\sum_{m=1}^{N}\int I(t)A_m \sin(\omega_m t + \varphi_m)h(t-\tau)d\tau\right|_{max} \end{aligned} \tag{9}$$

The pseudoacceleration response spectrum can be calculated by summation of a series of response spectra for single sinusoidal inputs. Thus, the response spectrum can be acquired by adding the curves in Fig. 8 for all the spectrum points considered. The only parameter in this procedure that we can control is the value A_m in Eq. (9). Therefore, in the low-frequency region and the peak RRS region, it is possible to control the CRS value to match the RRS value. However, if the RRS has a flat shape in the high-frequency region beyond the peak, as with the RRS in Fig. 5, it becomes even more difficult for the CRS to match the RRS. As shown in Fig. 8, the response

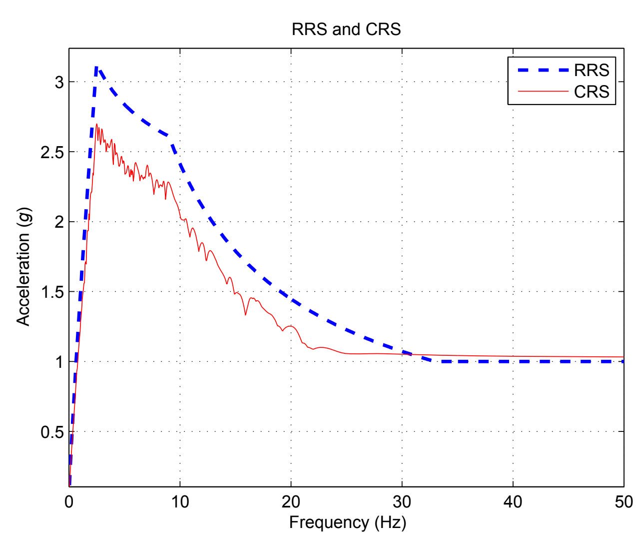

Fig. 5 – RRS and CRS by Eq. (6). CRS, calculated response spectrum; RRS, required response spectrum.

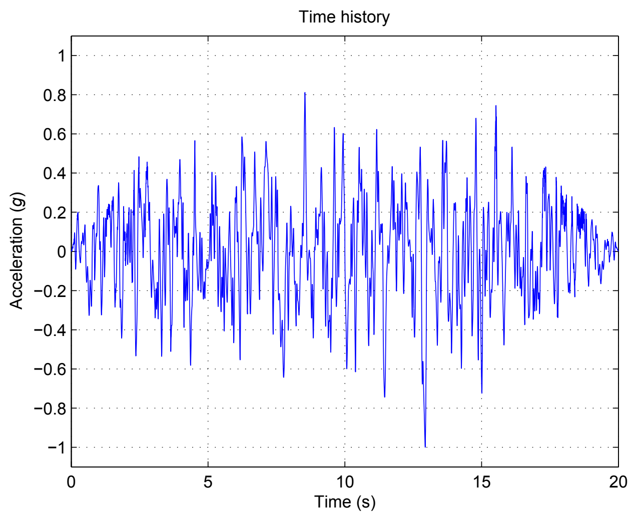

Fig. 6 – Artificial time history to get the CRS in Fig. 5. CRS, calculated response spectrum.

spectrum of a single sinusoidal input has an asymptote. This means that, unlike in a low-frequency region, a high-frequency CRS is formed by the summation of response spectra of single sinusoidal inputs with different natural frequencies. Hence, if a reference response spectrum has a shape similar to that of Fig. 8 (having an asymptote below unity in the high-frequency region), the CRS is not likely to approach the RRS. In this case, for the RRS in the high-frequency region has a fixed value of unity after 33 Hz (the cut-off frequency), it is difficult to have a CRS that approximates well with the RRS. Actually, as can be seen from Figs. 5 and 7, the CRS in the high-frequency region is greater than unity. Furthermore, during the iteration, to reduce the CRS in the high-frequency region, the overall set of $A_{n,k}$ in the time history $\ddot{x}(t)_k$ becomes smaller. However, this does not significantly affect the CRS in the high-frequency region, as stated above, while it considerably reduces the CRS in the low-frequency region and the RRS peak region. At the next iteration, to compensate for the reduction in the low-frequency and RRS peak regions, the overall set of $A_{n,k+1}$ takes on higher values and results in a higher CRS in the high-frequency region. At this stage, the peak of the time history becomes larger than unity. However, the maximum value of the time history must be compressed to unity to meet the first condition in Section 3.1. By scaling down the overall time history acceleration to force the peak to be unity, the overall CRS becomes smaller again.

Thus, a simple iterative process using Eq. (6) cannot produce a CRS that meets the conditions in Section 3.1. In this example, as can be seen from Figs. 5 and 7, the CRS in the high-frequency region (above 33 Hz) follows the RRS well. However, the CRS in the low-frequency region falls below 90% of the corresponding RRS. This means that the CRS in Fig. 5 fails to meet the fifth condition in Section 3.1.

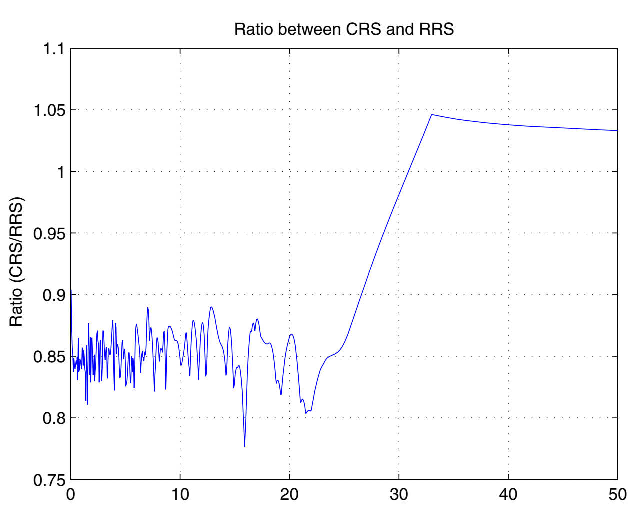

Fig. 7 – Ratio between RRS and CRS in Fig. 5. CRS, calculated response spectrum; RRS, required response spectrum.

4. Time-domain peak reduction method

4.1. *Conventional method for local response spectrum matching*

An artificial time history following a reference response spectrum can be generated as detailed in the last section. However, as can be seen from Figs. 5 and 7, just updating the overall coefficients, A_n, cannot produce a CRS curve that meets the conditions in Section 3.1. The calculated response in a certain frequency region can be much higher or lower than the corresponding RRS value, which does not meet the conditions in Section 3.1. Moreover, the values of A_n for obtaining the time history to get the CRS can diverge occasionally. To solve this, the frequencies at which the CRS is higher (peak) and lower (valley) than the RRS must be controlled. This means that the CRS must be controlled locally. In the case of a simple Fourier spectrum, the components of a certain frequency can be increased or reduced simply by raising or lowering the corresponding frequency contents of the input signal. However, in case of a response spectrum, controlling the local frequency

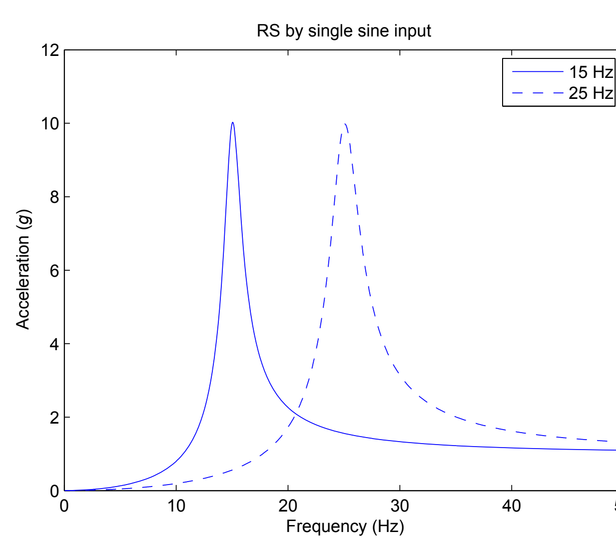

Fig. 8 – Response spectra for 15 Hz and 25 Hz sine inputs.

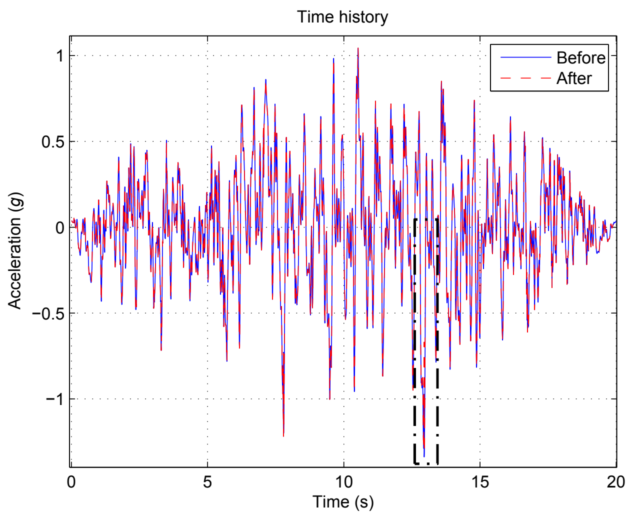

Fig. 9 – **Time history before and after time-domain peak reduction.**

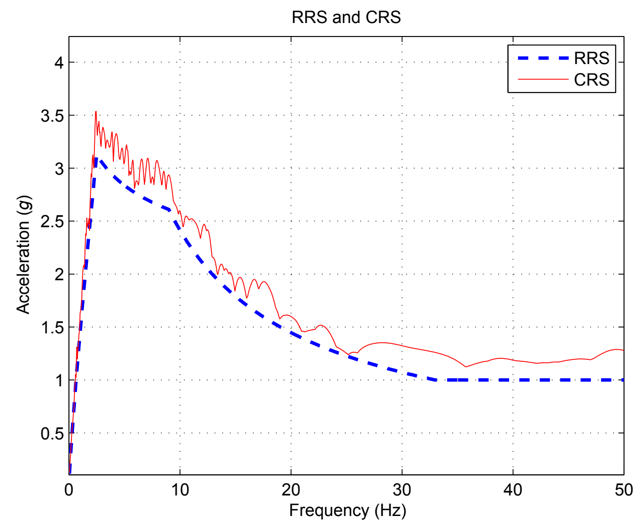

Fig. 11 – **RRS and CRS by time-domain peak reduction method. CRS, calculated response spectrum; RRS, required response spectrum.**

region is not an easy task. In this case, because we cannot control the one-dof system, we can control only the coefficients, A_n, of each sinusoid in the time history input. However, as mentioned in the works of Kost et al. [1] and Tsai [4], the response spectrum at a certain frequency cannot be controlled by just controlling the corresponding frequency component of the input time history. This is because a response spectrum is generated not only from the input time history, but also from the series of one-dof impulse responses. This means that even if a certain frequency value of the input is changed, the convolution integral with the series of one-dof systems that do not resonate with that frequency can still generate almost the same value as before.

To overcome this, Vanmarcke [6] used a power spectral density relation based on random vibration theory, which is somewhat complicated to understand. On the other hand, Kost et al. [1] and Tsai [4] proposed a deterministic method. They used the local control of the response spectrum by lowering and raising it at a central frequency and the adjacent frequency region. For the region where the CRS exceeds the RRS, Tsai [4] and Kost et al. [1] used a band stop filter to lower the frequency region:

$$|H_y| = \sqrt{\frac{\left(1-\Omega^2\right)^2 + (2\xi\Omega)^2}{\left[\left(1-\Omega^2\right)^2 + \frac{\Omega}{F}(2\xi\Omega)\right]^2 + \left[2\xi\Omega + \frac{\Omega}{F}\right]^2}} \tag{10}$$

where $\Omega = \omega/\omega_n$, $\xi =$ fraction of critical damping

For the region where the CRS is lower than the RRS, a method to raise the response using one-dof system impulse responses is suggested by Tsai [4] and Kost et al. [1]. However, as Tsai [4] pointed out, the suppression method using the band stop filter in Eq. (10) is not easy. To obtain the desired

Fig. 10 – **Time history before and after time-domain peak reduction (detailed view).**

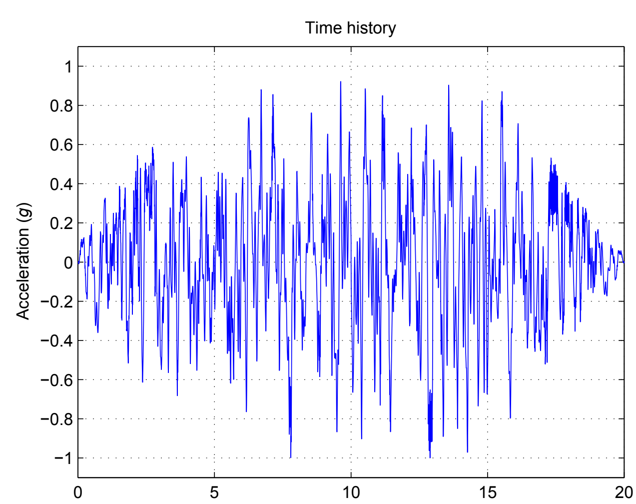

Fig. 12 – **Artificial time history to get the CRS in Fig. 11. CRS, calculated response spectrum.**

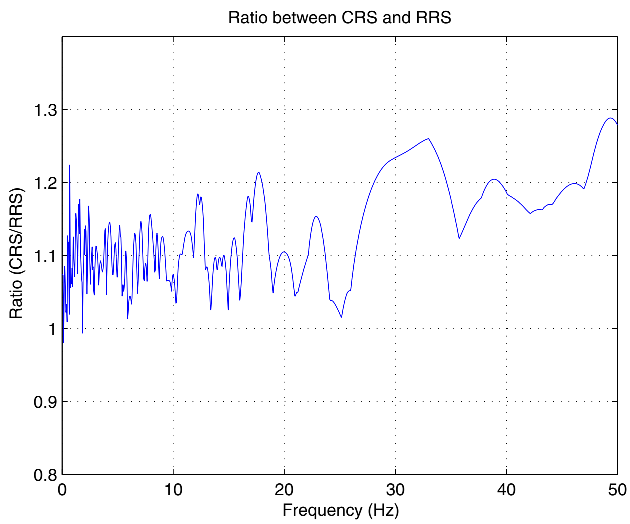

Fig. 13 – Ratio between RRS and CRS by the time-domain peak reduction method. CRS, calculated response spectrum; RRS, required response spectrum.

CRS using the band stop filter method, a trial-and-error approach with different F and ξ parameters is necessary. Thus, it is not a simple task to find adequate values of F and ξ simultaneously to obtain the desired CRS.

4.2. *Time-domain peak reduction method for response spectrum matching*

To avoid the complicated random vibration method and a tedious trial-and-error approach, a new method, called time-domain peak reduction, is suggested in this paper. As mentioned in the previous section, the response spectrum calculated from the time history by simply using Eq. (6) does not approximate the RRS well. This is because some of the peaks in the time domain exceed the others by a substantial amount. For example, in Fig. 6, except for the highest peak at approximately 13 seconds, the values of the highest peaks are at around 0.7g and 0.8g. Again, if we delete the peaks at around 8 seconds, 12.5 seconds, 15 seconds, and 15.5 seconds, the values of the next highest peaks will be about 0.6g. Thus, the occurrence of some number of excessively high peaks caused the gap between the low- and high-frequency response spectra.

To solve this problem, the excessively high peak accelerations in the time history data are reduced to become less than unity. Fig. 9 is an example of the time history data after the calculation of $A_{n,k+1}$ using Eq. (8). As can be seen from this figure, the highest peak has become larger than 1g. Additionally, there are just a few high peaks, while other values are at lower acceleration values. To cope with this, the accelerations at the highest peaks are reduced, as shown in the next few figures. The graph in Fig. 10 is a detailed view of the "dash–dot" box in Fig. 9. By carrying out the time-domain peak reduction and iteratively calculating $A_{n,k+1}$ using Eq. (8), one can obtain the final artificial time history.

4.3. *Result by time-domain peak reduction method*

Fig. 11 shows the final CRS calculated by the time-domain peak reduction method. Fig. 12 is the final artificial time history that produces the CRS in Fig. 11. The ratio between the CRS in Fig. 11 and the RRS is shown in Fig. 13. The figure shows that the CRS is higher than 90% of the RRS for all frequencies between 0.1 Hz and 50 Hz. The CRS falls below the RRS in two frequency windows, at approximately 1 Hz and 4.5 Hz. Both have two points that fall below the RRS. This shows that the CRS meets the fifth condition in Section 3.1. Lastly, the CRS is smaller than 130% of the RRS for all frequencies up to 50 Hz, satisfying the sixth condition in Section 3.1.

As a result, the time history in Fig. 10 meets all six conditions in Section 3.1. Thus, it has been demonstrated that an artificial time history can be generated using a simple time-domain peak reduction method to match a given reference response spectrum and to meet the six conditions derived from nuclear regulatory guidance. Furthermore, the amplitudes of the time histories that are generated using this

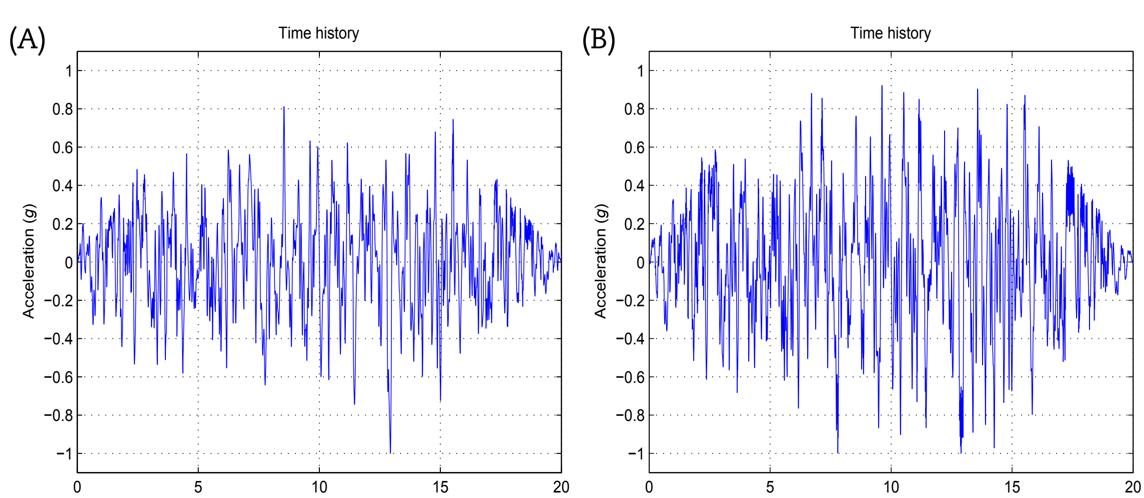

Fig. 14 – Artificial time histories. (A) The time histories without time-domain peak reduction. (B) The time histories with time-domain peak reduction

method are richer in the strong motion duration. This can easily be seen in Fig. 14, which shows artificial time histories with and without the time-domain peak reduction method generated from the same initial time history. The graph in Fig. 14B shows richer acceleration peak values across the entire time range considered, especially in the strong motion duration. Thus, the time history in graph in Fig. 14B contains a richer strong motion. By contrast, the graph in Fig. 14A contains just a few peaks in the strong motion duration. Therefore, by just applying an envelope function, we can hardly get signals with "strong and rich" peaks through the strong motion duration. This is another advantage of using the time-domain peak reduction method.

5. Conclusion

Due to the characteristics of response spectra for base excitation, the CRS in the high-frequency range tends to become higher in the case of a reference response spectrum with a high-frequency asymptote. An example of such a reference response spectrum can be found in Regulatory Guide 1.60. To generate an artificial time history that matches well with this reference response spectrum, a new method, called time-domain peak reduction, is presented. The method does not require complicated random vibration and probability theory, or tedious trial-and-error tasks. It has been shown that both the time history and the corresponding response spectrum generated by this new method satisfy conditions derived from regulatory guidance specified in SRP 3.7.1. Moreover, it has been shown that the time history generated by this method has a richer strong motion duration than a time history generated without this method.

Conflicts of interest

All authors have no conflicts of interest to delcare.

Acknowledgments

This work was supported by the research fund of Chungnam National University, Daejeon, Korea.

REFERENCES

[1] G. Kost, T. Tellkamp, H. Kamil, A. Gantayat, F. Weber, Automated generation of spectrum-compatible artificial time histories, Nucl. Eng. Des. 45 (1978) 243–249.

[2] S. Levy, J.P.D. Wilkinson, Generation of artificial time-histories, rich in all frequencies, from given response spectra, Nucl. Eng. Des. 38 (1976) 241–251.

[3] D.H. Jun, H.K. Pak, Y.B. Kim, Simulation of artificial ground accelerations to be used for seismic response analysis of building structures, Proc. Earthquake Eng. Soc. Korea 49 (1992) 111–120.

[4] N.C. Tsai, Spectrum-compatible motions for design purposes, J Eng Mech Div Proc ASCE 98 (1972) 345–356.

[5] P.C. Rizzo, D.E. Shaw, S.J. Jarecki, Development of real/synthetic time histories to match smooth design spectra, Nucl. Eng. Des. 32 (1975) 148–155.

[6] E.H. Vanmarcke, Structural response to earthquake, Chapter 8, in: C. Lomnitz, E. Rosenblueth (Eds.), Seismic Risk and Engineering Decisions, Elsevier Scientific Publishing Co., New York, 1976, pp. 287–337.

[7] D.A. Gasparini, E.H. Vanmarcke, SIMQKE, A Program for Artificial Motion Generation: User's Manual and Documentation, Department of Civil Engineering, MIT, USA, 1976.

[8] T.S. Aziz, J.K. Biswas, Spectrum-compatible time-histories for seismic design of nuclear power plants, Proceedings of the Third Canadian Conference on Earthquake Engineering, Vol. 1, 1979, pp. 301–324. Montreal.

[9] R.W. Clough, J. Penzien, Dynamics of Structures, third ed., Computers & Structures, Inc., Berkeley (CA), 2003.

[10] Design Response Spectra for Seismic Design of Nuclear Power Plants, Regulatory Guide 1.60 (Revision 1), US Nuclear Regulatory Commission, Washington D.C. (WA), 1973.

[11] Seismic Design Parameters, NUREG-0800, Standard Review Plan 3.7.1 (Revision 3), US Nuclear Regulatory Commission, Washington D.C. (WA), 2007.